American Mineralogist, Volume 89, pages 1130–1137, 2004

Raman spectroscopy of basic copper(II) and some complex copper(II) sulfate minerals: Implications for hydrogen bonding

RAY L. FROST,[1,*] PETER A. WILLIAMS,[2] WAYDE MARTENS,[1] PETER LEVERETT,[2] AND J. THEO KLOPROGGE[1]

[1] Inorganic Materials Research Program, Queensland University of Technology, GPO Box 2434, Brisbane Queensland 4001, Australia
[2] School of Science, Food and Horticulture, University of Western Sydney, Locked Bag 1797, Penrith South DC NSW 1797, Australia

ABSTRACT

Raman spectroscopy has been applied to the study of basic Cu sulfates including antlerite, brochiantite, posnjakite, langite, and wroewolfeite and selected complex Cu sulfate minerals. Published X-ray diffraction data were used to estimate possible hydrogen bond distances for the basic Cu sulfate minerals. A Libowitzky empirical expression was used to predict hydroxyl-stretching frequencies and agreement with the observed values was excellent. This type of study was then extended to complex basic Cu sulfates: cyanotrichite, devilline, glaucocerinite, serpierite, and ktenasite. The position of the hydroxyl-stretching vibration was used to estimate the hydrogen bond distances between the OH and the SO_4 units. The variation in bandwidth of the OH-stretching bands provided an estimate of the variation in these hydrogen bond distances. By plotting the hydrogen bond O···O distance as a function of the position of the SO_4 symmetric stretching vibration, the position of the SO_4 symmetric stretching band was found to be dependent upon the hydrogen bond distance for both the basic Cu sulfates and the complex Cu sulfates.

INTRODUCTION

Studies of the basic Cu sulfate minerals have existed for some time (Fowles 1926; Richmond and Wolfe 1940; Ungemach 1924). Such minerals are formed under specific conditions of pH and sulfate ion concentration. The minerals in this group are dolerophanite Cu_2OSO_4 (Richmond and Wolfe 1940), antlerite $Cu_3SO_4(OH)_4$ (Araki 1961; Finney and Araki 1963), brochantite $Cu_4SO_4(OH)_6$ (Helliwell and Smith 1997), and posnjakite $Cu_4SO_4(OH)_6{\cdot}H_2O$, langite $Cu_4SO_4(OH)_6{\cdot}2H_2O$, and wroewolfeite $Cu_4SO_4(OH)_6{\cdot}2H_2O$ (Pollard et al. 1990). Antlerite is more stable under acidic conditions than is brochantite. The temperature of crystallization is significant in the synthesis of these minerals, with posnjakite formed at lower temperatures than brochantite.

These minerals have been studied for various reasons: (1) as possible materials for the restoration of frescoes (Bersani et al. 2001); (2) corrosion and restoration of copper and bronze objects (Kratschmer et al. 2002; Livingston 1991; Lobnig et al. 1999; Mankowski et al. 1997; Matsuda et al. 1997; Nord et al. 1998; Bouchard-Abouchacra 2001); (3) corrosion of copper pipes containing reticulated water; (4) formation of these types of minerals in volcanic sublimations (Vergasova et al. 1988, 1984); and (5) formation of these types of minerals as leachates from slag dumps (Ruesenberg and Paulis 1996; Wappler and Tischendorf 1980).

Recent work by Bouchard-Abouchacra (2001) using Raman microscopy identified brochantite and antlerite on the corroded surface of a bronze object. Bouchard-Abouchacra (2001) also was able to distinguish the minerals malachite, azurite, brochantite and antlerite. Other minerals can be formed during Cu and Pb corrosion including nakaurite $Cu_4(SO_4)_4(CO_3)(OH)_6{\cdot}48H_2O$ and the mixed Cu-Pb species such as chenite $CuPb_4(SO_4)_2(OH)_6$, elyite $CuPb_4(SO_4)(OH)_8$, and caledonite $Cu_2Pb_5(SO_4)_3(OH)_6$ (Bouchard-Abouchacra 2001). Minerals such as chalcocyanite ($CuSO_4$) and dolerophanite (Cu_2OSO_4) will not form in any atmosphere containing moisture but may form in association with volcanic eruptions such as at Vesuvius in 79 AD, for example.

Many complex copper(II) sulfate systems exist with quite complex stoichiometry (Effenberger 1985, 1988; Effenberger and Zemann 1984). The complexity of these minerals results from the presence of a wide range of cations in the structure (Giuseppetti and Tadini 1987; Hess et al. 1988; Mellini and Merlino 1978; Mereiter 1982) and is reinforced by the presence of many multi-anion species. These anions include nitrate, phosphate, arsenate, carbonate, and hydroxyl (Orlandi and Perchiazzi 1989; Pierrot and Sainfeld 1961; Von Hodenberg et al. 1984; Zubkova et al. 2002).

Recently, the authors have applied Raman spectroscopy to the study of minerals containing oxyanions, including the elucidation of the structures of some basic Cu phosphate and sulfate minerals (Frost et al. 2002b). The single-crystal Raman spectra of azurite (Frost et al. 2002a), and the Raman spectra of the descloizite series and mottramite, were obtained at 298 and 77 K (Frost et al. 2001). Raman spectroscopy has also been used to study the mixed anionic mineral chillagite (Crane et al. 2002). In addition, the vibrational spectra of some naturally occurring pseudoalums have been determined (Frost et al. 2000). Recently, studies of the Raman spectroscopy of the vivianite phosphates and sulfates have been undertaken. It has proven extremely powerful for studying hydrated (such as the vivianite minerals), hydroxylated (basic Cu sulfates and phosphates) sulfated (natural alums)

* E-mail: r.frost@qut.edu.au

minerals. It seems apparent that few if any comprehensive Raman studies have been carried out on these basic Cu sulfate and complex basic Cu sulfate minerals. The objective of this research is the study of the relationship between hydrogen-bond distances and the position of the SO_4- and OH-stretching vibrations in the Raman spectra of the selected sulfates.

Experimental methods

Minerals used in this study are listed in Table 1. The identity of each phase was confirmed using X-ray diffraction, and the compositions checked using EDX measurements. No elements heavier than O (other than S and Cu) were detected (apart from Ca for devilline).

Raman microprobe spectroscopy

The crystals of the minerals were placed and oriented on a polished metal surface on the stage of an Olympus BHSM microscope, which is equipped with 10× and 50× objectives. The crystals were oriented to provide maximum intensity. All crystal orientations were used to obtain the spectra. Power at the sample was measured as 1 mW. The incident radiation was scrambled to avoid polarization effects. The microscope is part of a Renishaw 1000 Raman microscope system, which also includes a monochromator, a filter system, and a Charge Coupled Device (CCD). Raman spectra were excited by a Spectra-Physics model 127 He-Ne laser (633 nm) at a nominal resolution of 4 cm^{-1} in the range between 100 and 4000 cm^{-1}. Repeated acquisitions using the highest magnification were accumulated to improve the signal to noise ratio in the spectra. Spectra were calibrated using the 520.5 cm^{-1} line of a silicon wafer. Spectroscopic manipulation such as baseline adjustment, smoothing and normalization were performed using the Spectracalc software package GRAMS (Galactic Industries Corporation, NH, USA). Band component analysis was undertaken using the Jandel "Peakfit" software package, which enabled the type of fitting function to be selected and allows specific parameters to be fixed or varied accordingly. Band fitting was done using a Gauss-Lorentz cross-product function with the minimum number of component bands used for the fitting process. The Gauss-Lorentz ratio was maintained at values greater than 0.7, and fitting was undertaken until reproducible results were obtained with squared correlations, r^2, greater than 0.995.

Table 1. List of mineral names, museum numbers, and localities

Minerals	Museum no.	Locality
Langite	D4379	Cornwall, U.K.
Brochantite	D20320	Chuquicamata, Chile
Brochantite	D28957	Bisbee, Arizona, U.S.A.
Antlerite	M33489	Antlerite, Chuquicamata, Chile
Posnjakite	M27302	Drakewalls adit, near Gunnislake, Cornwall, U.K.
		Wroewolfeite Univ. of Cardiff, Wales
Cyanotrichite	G14601	Maid of Sunshine Mine, Cochise County, Arizona, U.S.A.
Devilline	G17182	Spania Dolina, Czechoslovakia
Ktenasite	G24983	Glomsevo Kollen, Amot Modum, Norway
Serpierite	G4034	Laurium, Greece
Glaucocerinite	G17641	Maid of Sunshine Mine, Cochise County, Arizona, U.S.A.

Results and discussion

The basic copper sulfate minerals antlerite, brochiantite, posnjakite, and langite all contain OH groups that are hydrogen bonded to adjacent sulfate groups (Araki 1961; Galy et al. 1984; Gentsch and Weber 1984; Hawthorne et al. 1989; Helliwell and Smith 1997; Mellini and Merlino 1979). The minerals posnjakite and langite contain water molecules that are also involved in hydrogen bonding with the adjacent sulfate anions. Antlerite has four OH units in the structure; brochantite has six OH units, and therefore Raman spectroscopy enables the spectra of some of these units to be obtained. Both antlerite and brochantite have hydroxyl stretching bands at 3580 and 3480 cm^{-1}, as shown in Figure 1. Posnjakite and langite are hydrated congeners of brochantite and, hence, have additional bands in their spectra over and above those observed in the spectra of antlerite and brochantite that are attributable to water OH-stretching. Wroewolfeite is a dimorph of langite (Hawthorne and Groat 1985). Bands are observed for langite at 3405, 3372 and 3262 cm^{-1} and are assigned to these water vibrations. Two hydroxyl OH-stretching bands are observed at 3564 and 3588 cm^{-1}. Bouchard-Abouchacra (2001) reported the Raman spectrum of brochantite and observed bands at 3562 and 3585 cm^{-1}. However, in the spectrum reported by her for brochantite, additional bands were observed at 3370 and 3400 cm^{-1}. The spectrum corresponds to that of langite, and

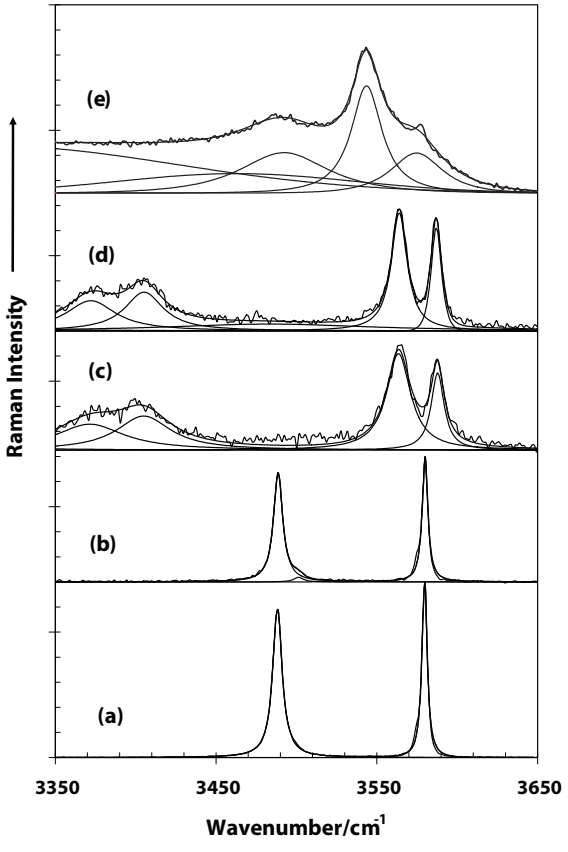

Figure 1. Raman spectrum of the hydroxyl-stretching region of (**a**) antlerite, (**b**) brochiantite, (**c**) posnjakite, (**d**) langite, and (**e**) wroewolfeite.

water bands are observed in the spectrum. The Raman spectrum reported for antlerite shows hydroxyl stretching bands at 3488 and 3580 cm^{-1}.

Several studies have shown a strong correlation between OH-stretching frequencies and both O···O bond distances and H···O hydrogen-bond distances (Emsley 1980; Lutz 1995; Mikenda 1986; Novak 1974). Libowitzky (1999), based upon the hydroxyl-stretching frequencies as determined by infrared spectroscopy, showed that the following regression function (with regression coefficients better than 0.96) can be employed to the above correlations:

$$\nu_1 = 3592–304 \times 109\exp[–d(\text{O-O})/0.1321]\ cm^{-1}$$

where d(O-O) is the bond distance.

Table 2 reports the hydrogen-bond distances for the basic sulfate minerals as calculated using available XRD data, together with the calculated OH-stretching frequencies and those observed by Raman spectroscopy. For antlerite, three hydrogen bonds are observed with distances of 3.188, 3.230, and 2.971 Å. By using Equation 1, predicted OH-stretching frequencies of 3582, 3585, and 3540 cm^{-1} were obtained. The observed hydroxyl-stretching frequencies are 3580 and 3488 cm^{-1}. The spectrometer cannot separate the two predicted bands at 3582 and 3580 cm^{-1}, and these will be observed as one band. The observed band at 3488 cm^{-1} does not match well with the predicted value of 3540 cm^{-1}. The reason for this mismatch is attributed to a bifurcated bond. A second reason for the mismatch is the geometry of hydrogen bonds. Such bonding is not necessarily linear.

For brochantite, six hydrogen bonds are observed with distances of 2.694, 3.131 (bifurcated), 3.059, 2.868, 2.919, and 3.021 Å. The last OH(6) group is not hydrogen bonded. The hydrogen-bond distance of 2.694 Å predicts an OH-stretching frequency of 3169 cm^{-1}. This band is not observed. Raman spectra are highly orientation dependent, and it is possible that this band was not observed for this reason. Hydrogen bond distances provide a predicted stretching frequency of 3565 cm^{-1}, which is close to that observed at 3580 cm^{-1}.

There are some 8 hydrogen bonds that can be predicted for the structure of wroewolfeite (Table 2). The O···O values all lie in the range 2.72 to 2.99 Å. It should also be noted that not all hydrogen atoms from OH units or water molecules form hydrogen bonds (bonds g, h, and i). Hydrogen bond a is of distance 2.72 Å, which, by using the Libowitzky type function, predicts a hydroxyl-stretching frequency of 3245 cm^{-1}. This band is observed at 3216 cm^{-1}, in good agreement with the predicted value. The second hydrogen bond (bond b) is 2.99 Å in length and a hydroxyl stretching frequency of 3547 cm^{-1} is predicted. A band at 3542 cm^{-1} is observed. Hydrogen bonds a and b are different in terms of the bond length that i being distinguished is the strength of the hydrogen bond, with bond a being strong and bond b significantly weaker. Such a distinction may be somewhat arbitrary. Any hydroxyl-stretching vibration above 3590 cm^{-1} results from weak hydrogen bonding. Bond c of distance 2.83 Å, predicts a value of 3441 cm^{-1}. However there is no observed band in this position. It is possible that the orientation of the crystal was such that the differential polarization vector did not align with the OH bond. The closest band is at 3325 or 3487 cm^{-1}. Bond d is 2.94 Å and a frequency of 3526 cm^{-1} is proposed, and a band is observed at 3542 cm^{-1}. What is also possible is that accidental degeneracy can occur. This accidental degeneracy results from the overlap of bands. The predicted bands combine to form a single broad band, as is observed in Figure 1 for wroewolfeite.

The crystal structure of langite has been published, but it is difficult to ascertain precise hydrogen bond positions without neutron scattering measurements (Galy et al. 1984; Gentsch and Weber 1984; Wappler 1971). The O···O distances are available from XRD data. From published data of langite, we predict some 13 possible hydrogen bonds and these are listed in Table 2. The system is complex and hydrogen-bond distances of 2.770 Å to

TABLE 2. Predicted Raman band frequencies of the hydroxyl stretching vibrations based upon the hydrogen-bond distances

	Bond	Hydrogen bonds (Å)	ν_1(calc)	ν_1(obs)
antlerite	a	OH1-O3 3.188(5)	3582	3580†
	b	OH2-O3 3.230(5)	3585	3580†
	c	OH3-O3 2.971(5)*	3540	3488
	d	OH3-O1 3.136(5)*		
Brochiantite	a	OH1-O8 2.694*	3169	*
	b	OH1-O9 3.131*	3565	3580†
	c	OH3-O9 3.059	3579	3489
	d	OH2-O6 2.868	3515*f*	3501*f*
	e	OH4-O9 2.919	3556*f*	3501*f*
	f	OH5-O9 3.021	3590	3580†
	g	OH6 is not H-bonded		
posnjakite	a	OH1-O11 2.746	3307	3372
	b	OH2-O10 2.732	3275	3262†
	c	OH3-O9 3.047	3563	3564
	d	OH4-O11 2.715	3231	3262†
	e	OH6-O9 2.737	3287	3262†
	f	OH8-O10 2.872, O(8) is the water molecule	3482	3405
	g	OH8-O11 3.189	3582	3588*f*
	h	OH5 is not H-bonded	3590	3588*f*
wroewolfeite	a	OH5-O12 2.72	3245	3216
	b	OH7-O2 2.99	3547	3542†
	c	OH9-O4 2.83	3441	3325?
	d	OH6-O1* 2.94	3526	3487
	e	OH6-O2* 2.87	3441	3325?
	f	OH8-O3 2.9	3503	3485
	g	OH10 not H-bonded	3590	3542
	h	Neither H on water O11 is H-bonded	3590	3542
	i	One H on water O12 is not H-bonded	3590	3542
langite	a	O1-O9 2.850	3462	
	b	O1-O12 3.115	3575	3564 or 3587
	c	O1-O8 3.156	3579	3564 or 3587
	d	O3-O12 2.770	3354	3372
	e	O3-O6 2.777	3366	3372
	f	O3-O7* 2.972	3540	3564
	g	O4-O7* 3.078	Not to be seen; bifurcation	
	h	O4-O11 2.889	3495	3564?
	i	O4-O12 2.884	3492	3564?
	j	OH not bonded	3592	3587
	k	O10-O12† 2.725	3258	3260
	l	a. O10-O11† 3.098	Not to be seen; bifurcation	
	m	b. O11-O12 2.869	3480	3405

Note: O5 to O10 are OH groups; O11 and O12 are water molecules. The former is bonded to a copper and the latter is a hydrogen-bonded lattice water molecule.
* Bifurcated; spectroscopic manifestation expected from the shorter interaction.
† Overlapped. f overlapped

3.156 Å (O-O) have been calculated. The hydrogen-bond distance of 2.770 Å is indicative of a strong hydrogen bond and this predicts hydroxyl-stretching frequencies of 3354 cm^{-1} (hydrogen bond d). Hydrogen-bond distances of 3.156 Å are indicative of weak hydrogen bonds and predicted frequencies approaching 3579 cm^{-1} have been obtained. Because of the flattening of the Libowitzky function in the high wavenumber region, little differences are observed in the predicted band positions for the weak hydrogen bonds.

In this work, we have used the Libowitzky function (Eq. 1) to ascertain the usefulness of comparing the hydroxyl-stretching vibrations and the sulfate SO_4-stretching vibrations to the O-H and O···O bond distances. We have then used the positions of the OH-stretching vibrations to predict hydrogen-bond distances for the OH units in the crystal structure for selected complex sulfates. In this way, we calculated the hydrogen-bond distances by the use of the Raman hydroxyl-stretching bands. The data in Table 2 fundamentally distinguish between types of OH units according to the H···O hydrogen-bond distances (Libowitzky 1999). That table shows a range of hydrogen-bond distances. These distances enable the calculation of the hydroxyl-stretching band positions. To the best of our knowledge, no neutron diffraction studies of these minerals have been forthcoming and hence no accurate hydrogen-bond H···O distances have been published. In this set of data, hydroxyl-stretching frequencies of the Raman spectra have been used to predict the hydrogen-bond distances for these minerals and, by using the band width of the hydroxyl-stretching frequencies, estimates of the variation in the hydrogen-bond distances have been predicted. No further attribution of the bonds can be made as the structures have not been determined.

The Raman spectra of the hydroxyl-stretching region of the selected multi-anionic minerals devilline, cyanotrichite, glaucocerinite, serpierite and, ktenasite are shown in Figure 2. Spectroscopic analysis of the data is reported in Table 3. The complex Cu sulfates contain two types of units capable of hydrogen bonding—namely the water molecule and the hydroxyl group. Three OH-stretching vibrations are observed in the Raman spectra of devilline at 3501, 3458, and 3456 cm^{-1}. The halfwidth values for these bands are 61.9, 16.4, and 87.0 cm^{-1}, respectively. The predicted hydrogen-bond distances for the devilline mineral are 2.89_7, 2.84_6, and 2.84_3 Å. No neutron diffraction data are available for comparison with these predicted values. Variation in the hydrogen-bond distances are ± 0.015, 0.009, and 0.517 Å, respectively. For cyanotrichite, four hydroxyl-stretching bands are observed at 3590, 3476, 3398, and 3198 cm^{-1}. Thus, hydrogen bonds are predicted to be 3.40_1, 2.86_5, 2.79_7, and 2.70_0 Å. It appears that the hydrogen bonds may be divided into strong and weak varieties according to the bond distance. Bonds of distance greater than 2.8 Å may be described as weak hydrogen bonds and bonds less than 2.8 Å as strong hydrogen bonds. The bandwidth of the Raman band indicates the variation in hydrogen-bond distance. The bandwidth of 59.0 cm^{-1} for the first OH-stretching band at 3590 cm^{-1} means that the variation in bond distance is $\pm 0.36_4$ Å. Greater variation is observed for the weak hydrogen bonds. The band at 3198 cm^{-1} attributed to a water OH-stretching vibration is broad with a bandwidth of 423 cm^{-1}. This corrresponds to a variation in bond distance of $\pm 0.65_3$ Å.

The complex sulfate mineral glaucocerinite shows two OH-stretching vibrations at 3471 and 3238 cm^{-1}, with bandwidths of 235 and 450 cm^{-1}. This yields hydrogen-bond distances of 3.980 and 2.717 Å, with variation of ±0.653 and ±0.133 Å, respectively. Again, two types of hydrogen bonds are distinguished according to the bond distance, namely weak (3.980 Å) and strong (2.717 Å) types. Greater variation in bond distance is observed for the weak hydrogen bonds. For the mineral serpierite, four hydroxyl stretching bands are observed at 3607, 3558, 3376, and 3198 cm^{-1} with bandwidths of 23.8, 85.5, 226, and 269 cm^{-1}. Hence, hydrogen-bond distances of 3.44_5, 3.026_9, 2.78_0, and 2.70_0 are predicted. For ktenasite, five hydroxyl stretching bands are observed at 3603, 3554, 3465, 3348, and 3187 cm^{-1} resulting in hydrogen-bond distances of 3.54_0, 3.01_0, 2.85_7, 2.76_6, and 2.69_9 Å.

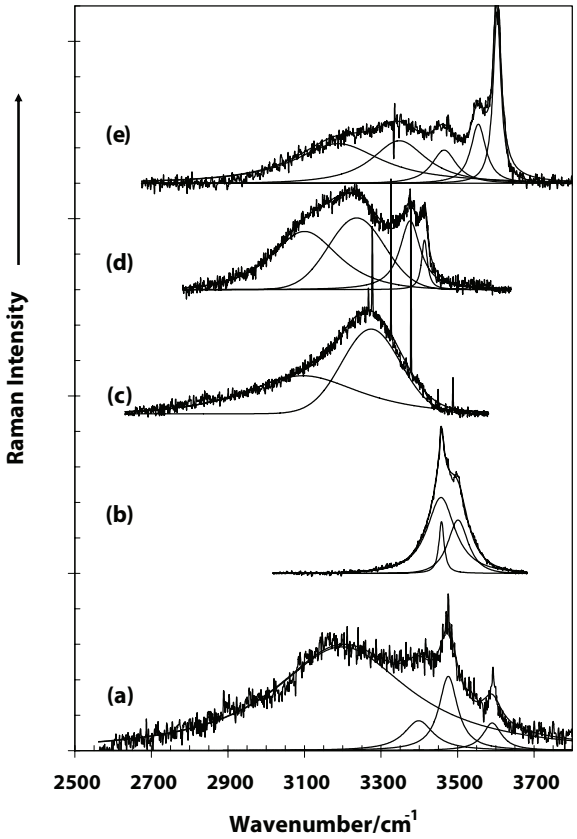

FIGURE 2. Raman spectrum of the hydroxyl-stretching region of (**a**) cyanotrichite, (**b**) devilline, (**c**) glaucocerinite, (**d**) serpierite, and (**e**) ktenasite.

Sulfate bands

The Raman spectroscopy of the aqueous sulfate tetrahedral oxyanion yields the symmetric stretching (ν_1) vibration at 981 cm^{-1}, the symmetric bending (ν_2) mode at 451 cm^{-1}, the antisymmetric stretching (ν_3) mode at 1104 cm^{-1}, and the antisymmetric bending (ν_4) mode at 613 cm^{-1}. The Raman spectrum of the mineral chalcanthite shows a single symmetric stretching mode at 984.7 cm^{-1}. Two ν_2 modes are observed at 463 and 445 cm^{-1}, and three ν_3 modes at 1173, 1146, and 1100 cm^{-1}. The ν_4 mode is observed as a single band at 610 cm^{-1}. A complex set

TABLE 3. Correlation between hydroxyl stretching frequencies and estimated hydrogen-bond distances

Mineral	Suggested hydrogen-bond origin*	Observed Raman band positions (cm^{-1})	Estimated hydrogen-bond distance (Å)	Observed Raman band width (cm^{-1})	Estimated hydrogen-bond distance variation (Å)
Devilline	OH 1	3501	2.89_7	61.9	$\pm 0.01_5$
	OH 2	3458	2.84_6	16.4	± 0.009
	H_2O 1	3456	2.84_3	87.0	$\pm 0.051_7$
Cyanotrichite	OH 1	3590	3.40_1	59.0	± 0.364
	OH 2	3476	2.86_5	59.0	$\pm 0.038_4$
	H_2O 1	3398	2.79_7	92.9	± 0.036
	H_2O 2	3198	2.70_0	423.7	$\pm 0.10_5$
Glaucocerinite	OH 1	3471	2.86_5	235.0	$\pm 0.065_3$
	H_2O 1	3238	2.71_7	450.0	± 0.133
Serpierite	OH 1	3607	3.44_5	23.8	± 0.100
	OH 2	3558	3.40_1	85.5	± 0.108
	H_2O 1	3376	2.78_0	226.2	$\pm 0.146_4$
	H_2O 2	3198	2.70_0	268.9	$\pm 0.035_6$
Ktenasite	OH 1	3603	3.44_1	24.7	$\pm 0.01_5$
	OH 2	3554	3.01	47.4	± 0.129
	H_2O 1	3465	2.85_7	76.4	± 0.043
	H_2O 2	3348	2.76_6	24.7	± 0.007
	H_2O 3	3187	2.69_9	27.5	± 0.060

* Assignments made according to the hydroxyl stretching wavenumber in the raman spectra.

of overlapping bands is observed in the low wavenumber region with broad bands observed at 257, 244, 210, 136, and 126 cm^{-1}. Recently, Raman spectra of four basic copper sulfate minerals, (antlerite, brochiantite, posnjakite, and langite) were published. The SO symmetric stretching modes for the four basic copper sulfate minerals are observed at 985, 990, 972, and 974 cm^{-1} respectively. Only the mineral brochantite showed a single band in this region. The Raman spectrum of antlerite shows bands at 990, 985, and 902 cm^{-1}, whereas posnjakite has bands at 972 and 905 cm^{-1}. Langite Raman spectrum shows complexity with overlapping bands observed at 982, 974, and 911 cm^{-1}. The observation of more than one symmetric SO_4-stretching vibration is attributed to a reduction in T_d symmetry. It should also be noted that each of the minerals displays a band(s) at around 1906 cm^{-1}. This band is attributed to the first overtone of the ν_1 symmetric stretching vibrations. Two bands are observed for langite at 1911 and 1906 cm^{-1}.

The two minerals posnjakite and langite show considerable complexity in the SO_4 antisymmetric stretching region whereas antlerite and brochantite show some similarity. The Raman spectrum of chalcanthite has the most intense band in this spectral region, centered at 1146 cm^{-1}. The Raman spectrum of antlerite shows bands at 1173, 1134, and 1078 cm^{-1} with the latter band being the most intense. A broad band centered at 1266 cm^{-1} is also observed for each of the minerals. The Raman spectrum of brochantite displays bands at 1173, 1135, and 1078 cm^{-1}. The Raman spectra of posnjakite and langite are very different from these of the former two minerals with a complex set of overlapping bands. The Raman spectrum of posnjakite shows bands at 1147, 1153, 1132, 1105, and 1078 cm^{-1} in the antisymmetric stretching region. In addition, bands are also observed at 1271 and 1251 cm^{-1}. An additional band is observed at around 1370 cm^{-1}. This band is common to all the spectra of these basic copper sulfate minerals, but of very low intensity for antlerite, brochantite, and chalcanthite. Raman bands for langite are observed at 1266, 1172, 1149, 1128, 1102 and 1076 cm^{-1}.

The Raman spectra of the SO symmetric and antisymmetric stretching vibrations of the complex Cu sulfates are shown in Figure 3. The results of the Raman spectroscopic analyses are shown in Table 4. The Raman spectrum of devilline shows a single SO_4 symmetric stretching bands at 1007 cm^{-1}. The band is sharp with a bandwidth of 3.1 cm^{-1}. The antisymmetric stretching band for devilline is observed at 1134 cm^{-1}. In contrast, the Raman spectrum of cyanotrichite shows a single intense band at 976 cm^{-1} with a broad low intensity band at 960 cm^{-1}. Three antisymmetric stretching bands are observed at 1137, 1101, and 1057 cm^{-1}. For glaucocerinite, bands are observed at 1007 and 981 cm^{-1} for the symmetric stretching vibrations and at 1129 and 1059 cm^{-1} for the antisymmetric stretching vibrations. For serpierite, a single symmetric stretching mode is observed at 988 cm^{-1} and three antisymmetric stretching bands are observed at 1131, 1122, and 1077 cm^{-1}. For ktenasite, multiple symmetric stretching bands are observed at 994, 981, and 973 cm^{-1}.

It is noted that the peak position of the sulfate band varies with the mineral. A plot of the hydrogen-bond distances, as predicted from the position of the OH-stretching vibration in the Raman spectrum, vs. the SO_4 symmetric stretching band position, yields the relationship shown in Figure 4. This graph shows quite conclusively that the position of the SO_4 stretching position is simply a function of the hydrogen-bond strength as determined by the hydrogen-bond distance. Two trends are observed, one for the simple basic copper sulfate minerals and another for the complex basic copper sulfate minerals. The two graphs parallel each other.

The complexity of the antisymmetric stretching region is reflected in the spectra of the ν_2 bending region (Fig. 5). The spectra of antlerite and brochantite are similar, in this spectral region, as are those for posnjakite and langite. The antlerite Raman spectrum shows bands at 485, 469, 440, and 415 cm^{-1} with the latter band having the highest intensity. Bouchard-Abouchacra (2001)

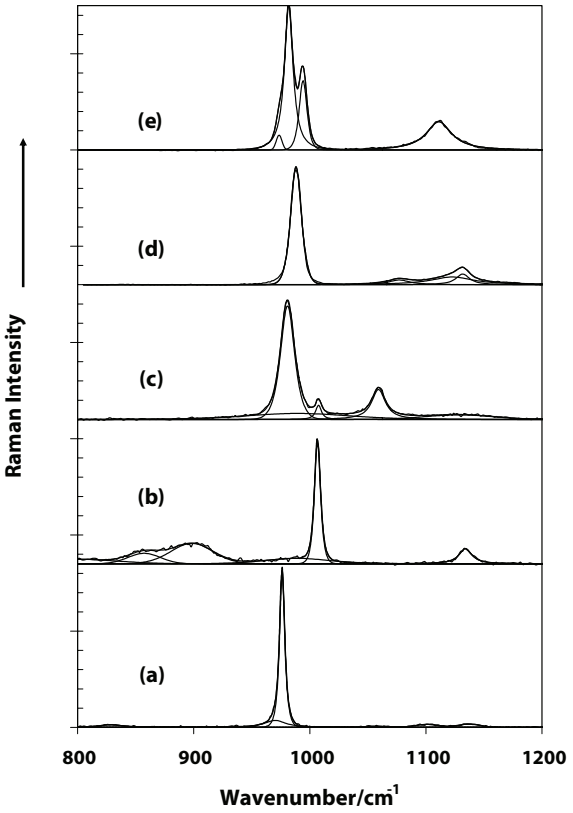

FIGURE 3. Raman spectrum of the SO_4-stretching region of (**a**) cyanotrichite, (**b**) devilline, (**c**) glaucocerinite, (**d**) serpierite, and (**e**) ktenasite.

TABLE 4. Raman spectroscopic analysis of some complex copper(II) sulfate minerals

Devilline	Cyano-trichite	Glaucocer-inite	Serpierite	Ktenasite
3501	3590	3471	3607	3603
3458	3476	3238	3558	3554
3456	3398		3376	3465
	3198		3198	3348
				3187
1134	1137	1129	1131	1111
	1101	1059	1122	1060
	1057		1077	
1007	976	1007		994
989		981	988	981
				973
898	828		843	710
857	829		806	
796	789		769	
668	594	694	645	604
617	530	613	605	
	510	555		
479	450	498	475	475
443	430	471	445	449
408			421	
324	365	256	332	397
	331		250	332
	277			

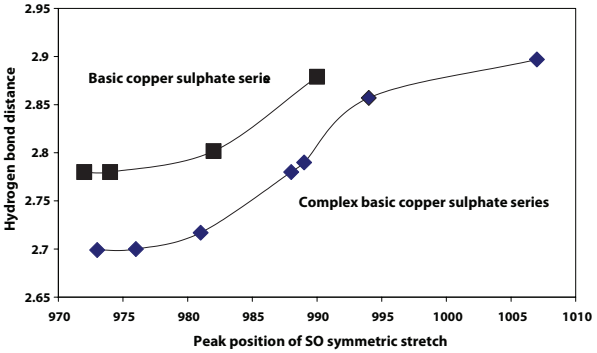

FIGURE 4. Hydrogen-bond distance as a function of the peak position of the symmetric SO_4-stretching vibration.

reported bands for antlerite at 483, 470, 444, and 416 cm^{-1}—in excellent agreement with our data. Raman spectra of brochantite are similar, except that additional bands are observed at 517 and 501 cm^{-1}. The Raman spectra of posnjakite show bands at 511, 482, 447, 422, 386, and 363 cm^{-1}. The complex set of bands in this region is also observed for langite, with bands observed at 507, 481, 449, 420, and 391 cm^{-1}. The Raman spectrum of wroewolfeite shows a complex set of overlapping bands at 472, 457, 443, and 415 cm^{-1}. The observation of additional bands over and above that which would be predicted for the sulfate anion (a single band at 451 cm^{-1}), may be attributed to several factors including symmetry reduction, local stress in the crystals, and crystal orientation effects.

Raman spectra of the mineral phases for this region are different, and each phase has its own characteristic spectrum. For antlerite, four Raman bands are observed at 651, 629, 606, and 600 cm^{-1}. Bouchard-Abouchacra found bands at 630 and 604 cm^{-1} for antlerite. In contrast, chalcanthite showed only a single band at 610 cm^{-1}. The Raman spectrum of brochantite shows bands at 629, 608, and 600 cm^{-1}. Bands were observed for brochantite by Bouchard-Abouchacra (2001) at 621, 611, and 599 cm^{-1}. The Raman spectrum of posnjakite shows bands at 621, 609, and 596 cm^{-1}, and langite at 621, 609, and 596 cm^{-1}. Although the bands for posnjakite and langite are in similar positions, the intensity of the bands varies considerably, but this may be a crystal orientation effect. The Raman spectrum of wroewolfeite shows two bands at 621 and 600 cm^{-1}.

The Raman spectra of the low wavenumber region of the selected Cu complex minerals are shown in Figure 6 and the results reported in Table 4. Multiple bands are observed in the 400 to 500 cm^{-1} region and are attributed to the ν_2 bending modes. The observation of several bending modes is in agreement with the number of antisymmetric stretching vibrations. Bands are observed at 479, 443, and 408 cm^{-1} for cyanotrichite, at 450 and 430 cm^{-1} for devilline, 498 and 471 cm^{-1} for glaucocerinite, at 475, 445, and 421 cm^{-1} for serpierite, and at 475 and 449 for ktenasite. The bands in the 500 to 600 cm^{-1} region are attributed to the ν_4 bending modes. Bands below 400 cm^{-1} are attributed to lattice modes. The Raman spectrum of ktenasite shows a single peak in the ν_4 region at 604 cm^{-1}. The Raman spectrum of devilline shows two low-intensity bands at 668 and 617 cm^{-1}; cynaotrichite shows two overlapping bands at 594 and 530 cm^{-1}; glaucocerinite

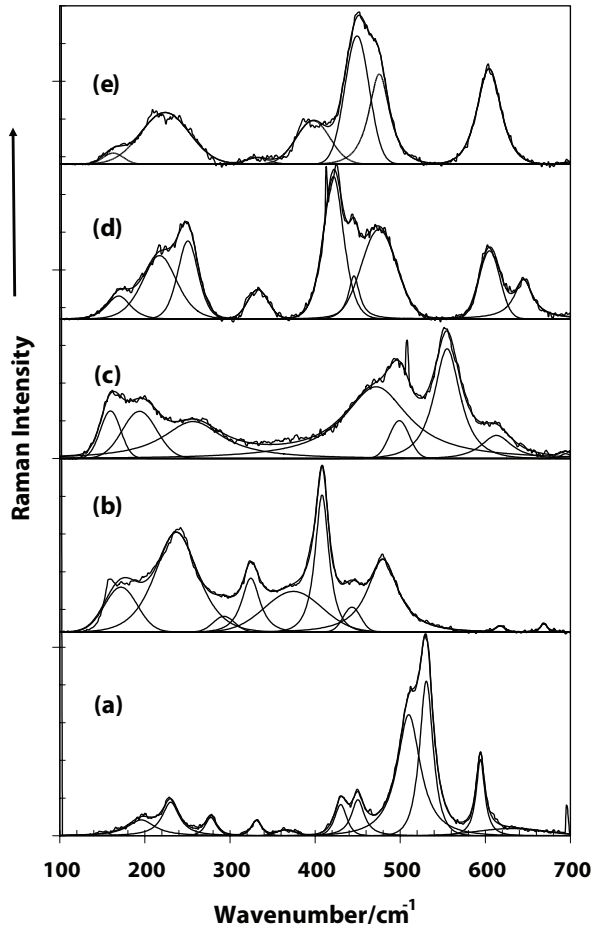

FIGURE 5. Raman spectrum of the SO_4 bending region of (**a**) antlerite, (**b**) brochiantite, (**c**) posnjakite, (**d**) langite, and (**e**) wroewolfeite.

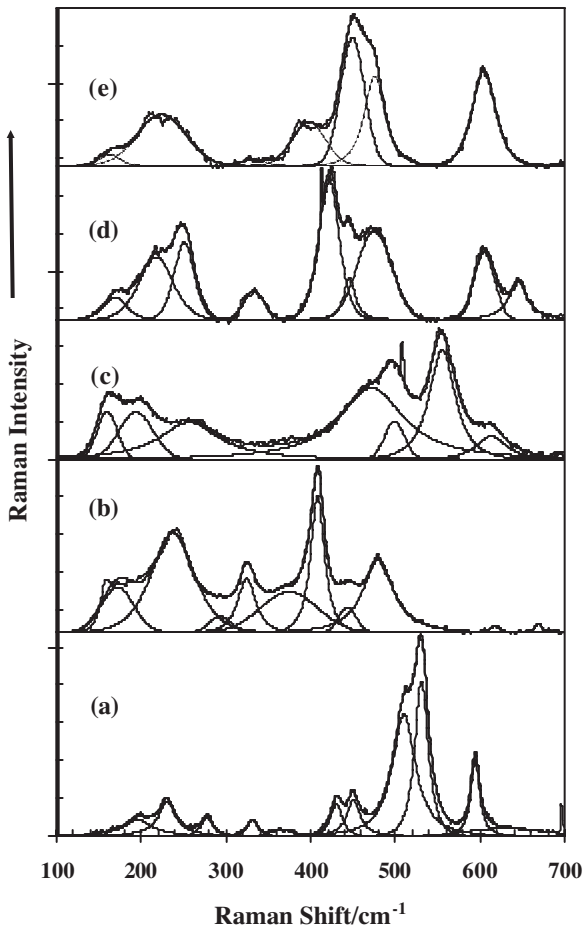

FIGURE 6. Raman spectrum of the low wavenumber region of (**a**) cyanotrichite, (**b**) devilline, (**c**) glaucocerinite, (**d**) serpierite, and (**e**) ktenasite.

shows three bands at 694, 613, and 555 cm^{-1}. The complexity of the symmetric and antisymmetric bending region shows a reduction in symmetry for these complex sulfate minerals.

The basic Cu sulfate minerals are characterized by the position of the hydroxyl stretching vibrations in the Raman spectrum. In addition, the minerals posnjakite and langite displayed four water OH-stretching vibrations. By using a Libowitzky type function (cf., Eq. 1), the hydrogen-bond distances were used to predict the hydroxyl-stretching frequencies and a comparison made to the observed values. Agreement is excellent. The position of the hydroxyl-stretching bands of the complex Cu sulfate minerals was used to estimate the hydrogen-bond distances in the mineral structures. A comparison was made between these hydrogen-bond distances and the position of the SO_4 symmetric stretching vibration.

ACKNOWLEDGMENTS

The infra-structure support of the Inorganic Materials Research Program of the Queensland University of Technology School of Physical and Chemical Sciences is gratefully acknowledged. The Australian Research Council (ARC) is thanked for funding. Allan Pring of the South Australian Museum is thanked for the loan of the basic complex copper sulfate minerals, as is also Ross Pogson of the Australian Museum. Dermot Henry of Museum Victoria is thanked for providing basic copper sulfate minerals, chiefly from Australian sources.

The authors wish to thank Eugen Libowitzky for his review of this manuscript and his most helpful and worthwhile comments.

REFERENCES CITED

Araki, T. (1961) Crystal structure of antlerite. Mineralogy Journal (Tokyo), 3, 233–235.

Bersani, D., Antonioli, G., Lottici, P.P., Fornari, L., and Castrichini, M. (2001) Restoration of a Parmigianino's fresco: a micro-Raman investigation of the pictorial surface. Proceedings of SPIE-The International Society for Optical Engineering, 4402, 221–226.

Bouchard-Abouchacra, M. (2001) Evaluation des capacites de la Microscopie Raman dans la caracterisation mineralogique et phsiochimique de materiaux archeologiques: metaux, vitraux et pigments. PhD Thesis. Museum National D'Histoire Naturelle, Paris.

Crane, M., Frost, R.L., Williams, P.A., and Kloprogge, J.T. (2002) Raman spectroscopy of the molybdate minerals chillagite (tungsteinian wulfenite-14), stolzite, scheelite, wolframite and wulfenite. Journal of Raman Spectroscopy, 33, 62–66.

Dunn, P.J., Rouse, R.C., and Nelen, J.A. (1975) Wroewolfeite, a new copper sulfate hydroxide hydrate. Mineralogical Magazine, 40, 1–5.

Effenberger, H. (1985) The crystal structure of mammothite, $Pb_6Cu_4AlSbO_2(OH)_{16}Cl_4(SO_4)_2$. Tschermaks Mineralogische und Petrographische Mitteilungen, 34, 279–88.

——— (1988) Ramsbeckite, $(Cu,Zn)_{15}(OH)_{22}(SO_4)_4.6H_2O$: Revision of the chemical formula based on a structure determination. Neues Jahrbuch für Mineralogie, Monatshefte, 38–48.

Effenberger, H. and Zemann, J. (1984) The crystal structure of caratiite. Mineralogical Magazine, 48, 541–6.

Emsley, J. (1980) Very strong hydrogen bonding. Chemical Society Reviews, 9, 91–124.

Finney, J.J. and Araki, T. (1963) Refinement of the crystal structure of antlerite. Nature, 197, 70.

Fowles, G. (1926) Basic copper sulfates. Journal of the Chemical Society,

1845–58.
Frost, R.L., Kloprogge, J.T., Williams, P.A., and Leverett, P. (2000) Raman microscopy of some natural pseudo-alums: halotrichite, apjohnite and wupatkiite, at 298 and 77 K. Journal of Raman Spectroscopy, 31, 1083–1087.
Frost, R.L., Williams, P.A., Kloprogge, J.T., and Leverett, P. (2001) Raman spectroscopy of descloizite and mottramite at 298 and 77 K. Journal of Raman Spectroscopy, 32, 906–911.
Frost, R.L., Martens, W.N., Rintoul, L., Mahmutagic, E., and Kloprogge, J.T. (2002a) Raman spectroscopic study of azurite and malachite at 298 and 77 K. Journal of Raman Spectroscopy, 33, 252–259.
Frost, R.L., Williams, P.A., Martens, W., Kloprogge, J.T., and Leverett, P. (2002b) Raman spectroscopy of the basic copper phosphate minerals cornetite, libethenite, pseudomalachite, reichenbachite and ludjibaite. Journal of Raman Spectroscopy, 33, 260–263.
Galy, J., Jaud, J., Pulou, R., and Sempere, R. (1984) Crystal structure of the langite $Cu_4[SO_4(OH)6H_2O]\cdot H_2O$. Bulletin de Mineralogie, 107, 641–8.
Gentsch, M. and Weber, K. (1984) Structure of langite, $Cu_4[(OH)_6|SO_4]\cdot 2H_2O$. Acta Crystallographica, C40, 1309–11.
Giuseppetti, G. and Tadini, C. (1987) Corkite, $PbFe_3(SO_4)(PO_4)(OH)_6$, its crystal structure and ordered arrangement of the tetrahedral cations. Neues Jahrbuch fuer Mineralogie Monatshefte, 71–81.
Hawthorne, F.C. and Groat, L.A. (1985) The crustal structure of wroewolfeite, a mineral with $[Cu_4(SO_4)(OH)_6(H_2O)]$ sheets. American Mineralogist, 70, 1050–1055.
Hawthorne, F.C., Groat, L.A., and Eby, R. (1989) Antlerite, $Cu_3SO_4(OH)_4$, a heteropolyhedral wallpaper structure. Canadian Mineralogist, 27, 205–210.
Helliwell, M. and Smith, J.V. (1997) Brochantite. Acta Crystallographica, C53, 1369–1371.
Hess, H., Keller, P., and Riffel, H. (1988) The crystal structure of chenite, $Pb_4Cu(OH)_6(SO_4)_2$. Neues Jahrbuch fuer Mineralogie Monatshefte, 259–64.
Kratschmer, A., Odnevall Wallinder, I., and Leygraf, C. (2002) The evolution of outdoor copper patina. Corrosion Science, 44, 425–450.
Libowitzky, E. (1999) Correlation of O-H stretching frequencies and O-H...O hydrogen bond lengths in minerals. Monatshefte für Chemie, 130, 1047–1059.
Livingston, R.A. (1991) Influence of the environment on the patina of the Statue of Liberty. Environmental Science and Technology, 25, 1400–8.
Lobnig, R., Frankenthal, R.P., Jankoski, C.A., Siconolfi, D.J., Sinclair, J.D., Unger, M., and Stratmann, M. (1999) Corrosion and protection of metals in the presence of submicron dust particles. Proceedings—Electrochemical Society, 99–29, 97–126.
Lutz, H. (1995) Hydroxide ions in condensed material—correlation of spectroscopic and structural data. Structure and Bonding (Berlin, Germany), 82, 85–103.
Mankowski, G., Duthil, J.P., and Giusti, A. (1997) The pit morphology on copper in chloride- and sulfate-containing solutions. Corrosion Science, 39, 27–42.
Matsuda, S., Aoki, S., and Kawanobe, W. (1997) Analysis of corrosion products formed on the bronze garden lantern of Todaiji Temple in Nara. Hozon Kagaku, 36, 1–27.
Mellini, M. and Merlino, S. (1978) Ktenasite, another mineral with $[(Cu,Zn)_2(OH)_3O]$-octahedral sheets. Zeitschrift für Kristallographie, 147, 129–40.
——— (1979) Posnjakite: $2[Cu_4(OH)_6(H_2O)O]$ octahedral sheets in its structure. Zeitschrift für Kristallographie, 149, 249–57.
Mereiter, K. (1982) The crystal structure of johannite, $Cu(UO_2)_2(OH)_2(SO_4)_2\cdot 8H_2O$. Tschermaks Mineralogische und Petrographische Mitteilungen, 30, 47–57.
Mikenda, W. (1986) Stretching frequency vs. bond distance correlation of O-D(H)...Y (Y = N, O, S, Se, Cl, Br, I) hydrogen bonds in solid hydrates. Journal of Molecular Structure, 147, 1–15.
Nord, A.G., Mattsson, E., and Tronner, K. (1998) Mineral phases on corroded archaeological bronze artifacts excavated in Sweden. Neues Jahrbuch für Mineralogie Monatshefte, 265–277.
Novak, A. (1974) Hydrogen bonding in solids. Correlation of spectroscopic and crystallographic data. Structure and Bonding (Berlin), 18, 177–216.
Orlandi, P. and Perchiazzi, N. (1989) Ramsbeckite, $(Cu,Zn)_{15}(OH)_{22}(SO_4)_4\cdot 6H_2O$, a first occurrence for Italy from "La Veneziana" mine, Valle dei Mercanti, Vicenza. European Journal of Mineralogy, 1, 147–9.
Pierrot, R. and Sainfeld, P. (1961) Devillite and spangolite of Corsica. The associated minerals. Bulletin De La Societe Francaise Mineralogie et de Cristallographie, 84, 90–1.
Pollard, A.M., Thomas, R.G., and Williams, P.A. (1990) Mineralogical changes arising from the use of aqueous sodium carbonate solutions for the treatment of archaeological copper objects. Studies in Conservation, 35, 148–52.
Richmond, W.E. and Wolfe, C.W. (1940) Crystallography of dolerophanite. American Mineralogist, 25, 606–10.
Ruesenberg, K.A. and Paulis, P. (1996) Conversions and new formations in slag dumps of the Pribram lead and silver foundry, Czech Republic. Aufschluss, 47, 267–287.
Ungemach, H. (1924) Antlerite. Bulletin De La Societe Francaise Mineralogie Et De Cristallographie, 47, 124–9.
Vergasova, L.P., Filatov, S.K., Serafimova, E.K., and Starova, G.L. (1984) Piypite, $K_2Cu_2O(SO_4)_2$—a new mineral of volcanic sublimates. Doklady Akademii Nauk, 275, 714–17.
Vergasova, L.P., Filatov, S.K., Serafimova, E.K., and Semenova, T.F. (1988) Ponomarevite, $K_4Cu_4OCl_{10}$—a new mineral from volcanic sublimations. Doklady Akademii Nauk, 300, 1197–200.
Von Hodenberg, R., Krause, W., and Taeuber, H. (1984) Schulenbergite, $(Cu,Zn)_7(SO_4,CO_3)_2(OH)_{10}\cdot 3$ H2O, a new mineral. Neues Jahrbuch für Mineralogie Monatshafte, 17–24.
Wappler, G. (1971) Crystal structure of langite $Cu_4[(OH)_6/SO_4]\cdot H_2O$. Berichte der Deutschen Gesellschaft Geologische Wissenschaften Reihe B, 16, 175–203.
Wappler, G. and Tischendorf, G. (1980) Identification of some secondary minerals from the dumps of the Friedrichsglueck Mine, near Neustadt/Rennsteig [East Germany]. Zeitschrift Für Geologische Wissenschaften, 8, 1397–402.
Zubkova, N.V., Pushcharovsky, D.Y., Giester, G., Tillmanns, E., Pekov, I.V., and Kleimenov, D.A. (2002) The crystal structure of arsentsumebite, $Pb_2Cu[(As, S)O_4]_2(OH)$. Mineralogy and Petrology, 75, 79–88.

MANUSCRIPT RECEIVED DECEMBER 12, 2002
MANUSCRIPT ACCEPTED MAY 22, 2003
MANUSCRIPT HANDLED BY SIMON KOHN